# CLAS-ANALYSIS 2016

Dalitz Plot Analysis of $\eta' \rightarrow \eta\ \pi^+\ \pi^-$ from g12

## 1. Introduction

In this note we will explain the analysis details to obtain the Dalitz plot parameters of the decay of $\eta' \to \eta\, \pi^+\, \pi^-$ meson. The final state particles proton, $\pi^+$ and $\pi^-$ information from PART BOS bank are identified with the particle identification codes compiled in the "clas6-trunk" under the package CLASEVENT . We selected a data sample with all those events which has only one proton, $\pi^+$ and $\pi^-$ in their final state and no matter how many neutral particles.

We started the analysis with well calibrated data as ".root" files with all events arranged as per the Run number, Event number and PID along with all other informations recorded by the experiment. The calibrated data is then corrected and further processed following the steps of " g12 procedures working version.pdf " and properly tuned Kinematic Fitter available at G12 Wikki [1]. We have divided our analysis into the following subsequent sections.

- Event Selection : The Section 2 will cover analysis cut involved to tap the events of interest.
- Simulation : The Section 3 will explain our analysis model and will produce a cross check to the whole analysis
- Result : The Section 4 will report the final results of the measurement with a study of systematics.

The complete reaction under study is " $\gamma$ p $\to \eta'(\to \eta\, \pi^+\, \pi^-)$ p " and we do not detect $\eta$ meson. This is a missing mass analysis using a fixed target g12 experiment, which has an energy of the photon beam ranging from 1.142 GeV to 5.425 GeV. However the threshold production of $\eta'$ meson is 1.455 GeV and hence we analysed the data from the threshold to our maximum available energy.

## 2. Event Selection

We are interested in the photo-production of $\eta'$ meson and its decay to $\eta$, $\pi^+$ and $\pi^-$ mesons. The improvement in the identification of the particles, selection of an event and several cuts in the analysis to tap the events of interest is reported subsequent sub sections.

### 2.1. Run List

TABLE 1. List of runs included in the analysis

| G12 Run List | G12 Run List | G12 Run List | G12 Run List | G12 Run List |
|---|---|---|---|---|
| 56605 | 56653 | 56654 | 56655 | 56656 |
| 56660 | 56661 | 56665 | 56666 | 56667 |
| 56668 | 56669 | 56670 | 56673 | 56674 |
| 56688 | 56689 | 56690 | 56691 | 56692 |
| 56693 | 56694 | 56695 | 56696 | 56700 |
| 56701 | 56702 | 56703 | 56704 | 56705 |
| 56706 | 56707 | 56708 | 56710 | 56711 |
| 56712 | 56713 | 56714 | 56715 | 56716 |
| 56717 | 56718 | 56719 | 56720 | 56721 |
| 56722 | 56723 | 56724 | 56726 | 56727 |
| 56728 | 56729 | 56730 | 56731 | 56732 |
| 56733 | 56734 | 56735 | 56736 | 56737 |
| 56738 | 56739 | 56740 | 56741 | 56742 |
| 56743 | 56744 | 56748 | 56749 | 56750 |
| 56751 | 56752 | 56753 | 56754 | 56755 |
| 56756 | 56757 | 56758 | 56759 | 56760 |
| 56761 | 56762 | 56763 | 56764 | 56765 |
| 56766 | 56767 | 56768 | 56770 | 56771 |
| 56772 | 56774 | 56775 | 56776 | 56777 |
| 56778 | 56780 | 56781 | 56782 | 56783 |

| | | | | |
|---|---|---|---|---|
| 56784 | 56787 | 56788 | 56791 | 56792 |
| 56793 | 56794 | 56798 | 56799 | 56800 |
| 56801 | 56802 | 56805 | 56806 | 56807 |
| 56808 | 56809 | 56810 | 56811 | 56812 |
| 56813 | 56814 | 56815 | 56821 | 56822 |
| 56823 | 56824 | 56825 | 56826 | 56827 |
| 56831 | 56832 | 56833 | 56834 | 56838 |
| 56839 | 56841 | 56842 | 56843 | 56844 |
| 56845 | 56849 | 56853 | 56854 | 56855 |
| 56856 | 56857 | 56858 | 56859 | 56860 |
| 56861 | 56862 | 56864 | 56865 | 56866 |
| 56870 | 56874 | 56875 | 56877 | 56879 |
| 56897 | 56898 | 56899 | 56900 | 56901 |
| 56902 | 56903 | 56904 | 56905 | 56907 |
| 56908 | 56914 | 56915 | 56916 | 56917 |
| 56918 | 56919 | 56921 | 56922 | 56923 |
| 56924 | 56925 | 56926 | 56927 | 56928 |
| 56929 | 56930 | 56932 | 56935 | 56936 |
| 56937 | 56938 | 56939 | 56940 | 56948 |
| 56949 | 56950 | 56951 | 56952 | 56953 |
| 56954 | 56955 | 56956 | 56958 | 56960 |
| 56961 | 56962 | 56963 | 56964 | 56965 |
| 56966 | 56967 | 56968 | 56969 | 56970 |
| 56971 | 56972 | 56973 | 56974 | 56975 |
| 56977 | 56978 | 56979 | 56980 | 56992 |
| 56993 | 56994 | 56996 | 56997 | 56998 |
| 56999 | 57000 | 57001 | 57002 | 57003 |
| 57004 | 57005 | 57006 | 57008 | 57009 |
| 57010 | 57011 | 57012 | 57013 | 57014 |
| 57015 | 57016 | 57017 | 57021 | 57022 |

| | | | | |
|---|---|---|---|---|
| 57023 | 57025 | 57026 | 57027 | 57030 |
| 57031 | 57032 | 57062 | 57063 | 57064 |
| 57065 | 57066 | 57067 | 57068 | 57069 |
| 57071 | 57072 | 57073 | 57075 | 57076 |
| 57077 | 57078 | 57079 | 57080 | 57095 |
| 57096 | 57097 | 57100 | 57101 | 57102 |
| 57103 | 57106 | 57107 | 57108 | 57114 |
| 57115 | 57116 | 57117 | 57118 | 57119 |
| 57120 | 57121 | 57122 | 57123 | 57124 |
| 57125 | 57126 | 57127 | 57128 | 57130 |
| 57131 | 57132 | 57133 | 57134 | 57135 |
| 57136 | 57137 | 57138 | 57139 | 57140 |
| 57141 | 57142 | 57143 | 57144 | 57145 |
| 57146 | 57147 | 57148 | 57149 | 57150 |
| 57151 | 57152 | 57159 | 57160 | 57161 |
| 57162 | 57163 | 57164 | 57165 | 57166 |
| 57167 | 57168 | 57170 | 57171 | 57172 |
| 57173 | 57174 | 57175 | 57176 | 57177 |
| 57178 | 57179 | 57180 | 57181 | 57182 |
| 57183 | 57184 | 57185 | 57189 | 57190 |
| 57191 | 57192 | 57193 | 57194 | 57195 |
| 57196 | 57197 | 57198 | 57199 | 57200 |
| 57201 | 57202 | 57203 | 57204 | 57205 |
| 57206 | 57207 | 57208 | 57209 | 57210 |
| 57211 | 57212 | 57213 | 57214 | 57215 |
| 57216 | 57217 | 57218 | 57219 | 57220 |
| 57221 | 57222 | 57223 | 57224 | 57225 |
| 57226 | 57227 | 57228 | 57229 | 57233 |
| 57234 | 57235 | 57236 | 57249 | 57250 |
| 57251 | 57252 | 57253 | 57255 | 57256 |

| | | | | |
|---|---|---|---|---|
| 57257 | 57258 | 57260 | 57261 | 57262 |
| 57263 | 57264 | 57265 | 57266 | 57267 |
| 57268 | 57270 | 57271 | 57272 | 57274 |
| 57275 | 57276 | 57277 | 57278 | 57279 |
| 57280 | 57281 | 57282 | 57283 | 57284 |
| 57285 | 57286 | 57287 | 57288 | 57290 |
| 57291 | 57293 | 57294 | 57295 | 57296 |
| 57297 | 57298 | 57299 | 57300 | 57301 |
| 57302 | 57303 | 57304 | 57305 | 57306 |
| 57307 | 57308 | 57309 | 57310 | 57311 |
| 57317 | 57308 | 57309 | 57310 | 57311 |

### 2.2. Selection of the Beam Photon

In an event we found that multiple bremsstrahlung photons were recorded as the incident beam. The multiple beam photon arises from 2.004 beam bunching spacing of the electrons in the storage ring. These electrons gives the bremsstrahlung photons in the radiator and creates multiple hits in the trigger and thereby satisfying trigger logic to record them. In this analysis we selected all the photons which falls within the timing window of $|\text{Tagger Time - StartTime}| \leq 1.002$ ns, and consider each of them as an individual event.

### 2.3. Vetex Cut

In the g12 experiment the target was positioned -90 cm from the CLAS center. The target cell was 40 cm long and 2 cm in radius in the form of a cylinder filled with unpolarised liquid hydrogen. We used this target information and imposed it to all event vertexes. We required all events production vertex tracks to originate in the target region via the condition that $\sqrt{v_x^2 + v_y^2} \leq 2$ cm and -110 $\geq v_z \leq$ -70 cm.

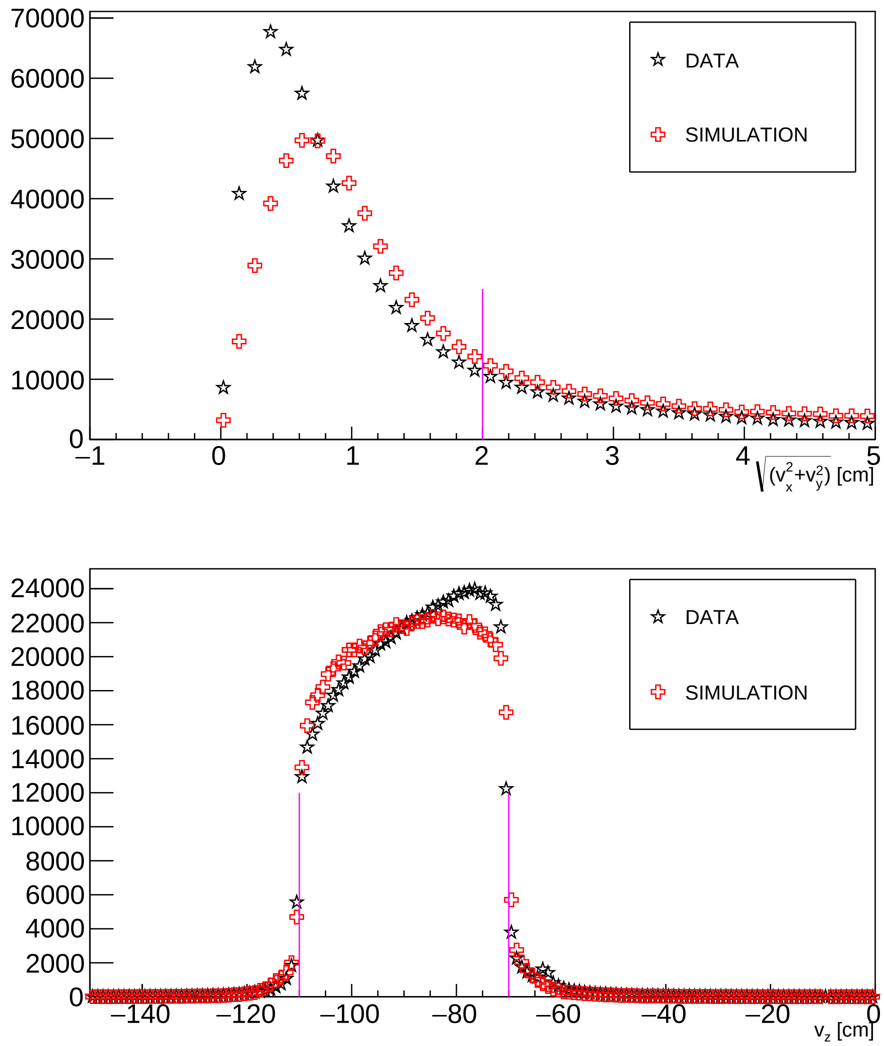


FIGURE 1. [tpho + tprop -scvt] distribution from the simulation and data for proton, $\pi^+$ and $\pi^-$.

### 2.4. Timing Cuts on proton, $\pi^+$ and $\pi^-$

As a post PID improvement of the detected final state particles $\pi^+$, $\pi^-$ and proton, we introduced a vertex timing ($t_{vert}$) cut of particles in the analysis. The $t_{vert}$, vertex time is the instant of time the particle left the target. One can calculate it through the information of the TOF detectors as,

$$t_{vert}(TOF) = t_{TOF} - \frac{l_{TOF}}{c\beta}$$

where $t_{TOF}$ and $l_{TOF}$ are the measured time and length of particle in TOF sub detector. Here c is the velocity of light in vacuum and $\beta$ is the Lorentz factor of the particle calculated by knowing the velocity(v) of particle as $\beta = \frac{v}{c}$. The same vertex timing ($t_{vert}$) information can also be calculated from the RF-corrected time instant of the photon ($t_{photon}$) crossing the target center measure by the tagger added with the $t_{prop}$, which is the propagation time from the center of the target to the track vertex. Given by,

$$t_{vert}(Tagger) = t_{photon} + t_{prop}.$$

The difference of the $t_{vert}(TOF)$ from $t_{vert}(Tagger)$ is shown in Fig. 2, and we make a cut of $\pm$ 1.0 ns around 0 ns for all the final state particles in both simulation and data.

## 3. G12 Corrections

The G12 Corrections were derived from the exclusive $\pi^+$, $\pi^-$ and proton reaction. We used the following corrections in the analysis [1]:

- Beam Energy Correction : Is a correction to the incident beam photon energy and dependent on the Run number of the event. This correction is only applicable data and not to the simulated events.
- Removal of bad TOF paddle : This correction takes the Sector number and Paddle number as input. We used the correction to remove only those paddles that shows a significant drift on the resolutions of particle.
- Geometric Fiducial Cut : This cut removes the dead part of the detector from the $\theta - \phi$ map of the particle. We used it with the "nominal" option.

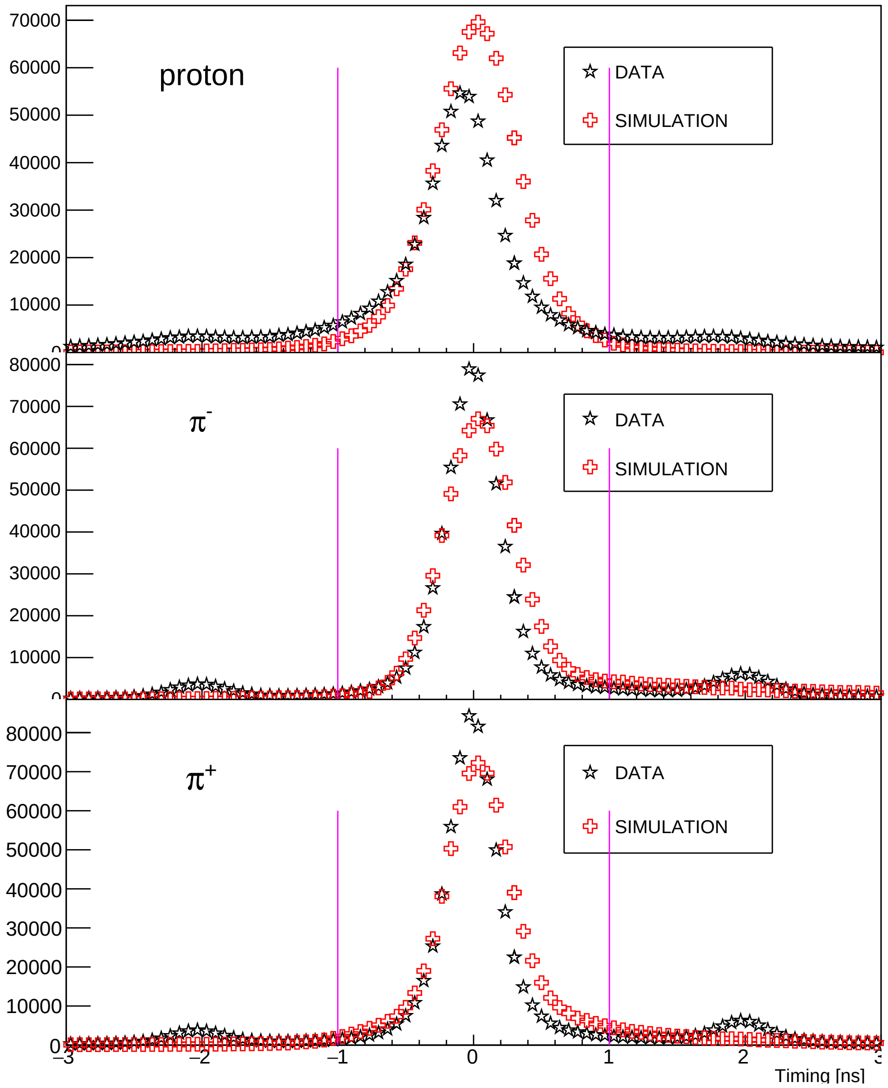


FIGURE 2. $[t_{vert}(TOF)$ - $t_{vert}(Tagger)]$ distribution from the simulation and data for proton(Upper), $\pi^+$(Middle) and $\pi^-$(Lower).

### 3.1. Kinematic Fitting

Kinematic fitter is a useful tool often used to get rid of unwanted background from signal channels and helps to improve the signal to background ratio. Any measurement with a tool comes with an error, and it can be represented as a vector $\vec{\eta}$. We can also define the measurement as

$\vec{\eta} = \vec{y}. + \vec{\epsilon}.$

Where the $\vec{y}$ and $\vec{\epsilon}$ denotes the actual value of the measurement without error and $\vec{\epsilon}$ is the error associated with the measurement. The kinematic information of a physics channel along with the constrains imposed allows the fitter to calculate the probability and $\chi^2$ of each event using Lagrange multipliers to perform a least-squares fit. The CLAS g12 Kinematic fitter takes the "TBER (Track Based Error)" matrix, vertex of information and lorentzvector of all particles as input, and returns Pull probabilities and $\chi^2$ for each events. The Pull probabilities when fitted with Guassian, its mean and $\sigma$ decides the quality of the covariance matrix and kinematic fit. In the ideal case of gaussian fitted to the Pulls of the particles should have zero mean and $\sigma$ of one, which ensures that the fitter correctly calculates covariance matrix error.

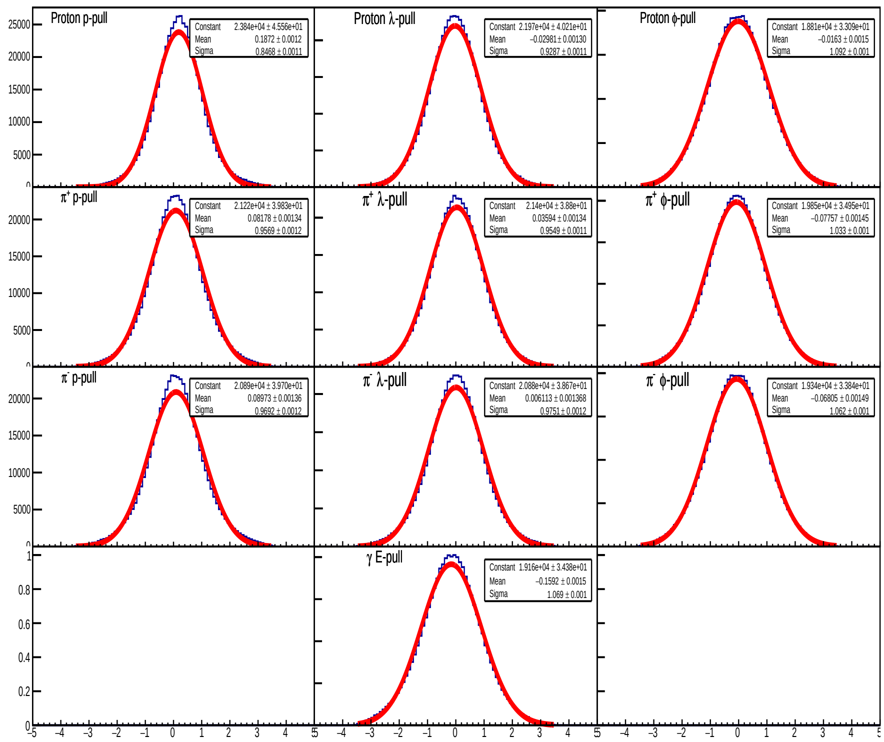


FIGURE 3. The Pull distributions for a (4-C) kinematic fit to $\gamma$ p $\rightarrow \pi^+$ $\pi^-$ p from g12 data with run 56655 after a 1% Pull probability cut.

The CLAS g12 Kinematic fitter is tuned for 4C constrained reaction,

$$\gamma p \rightarrow \pi^+\pi^- p.$$

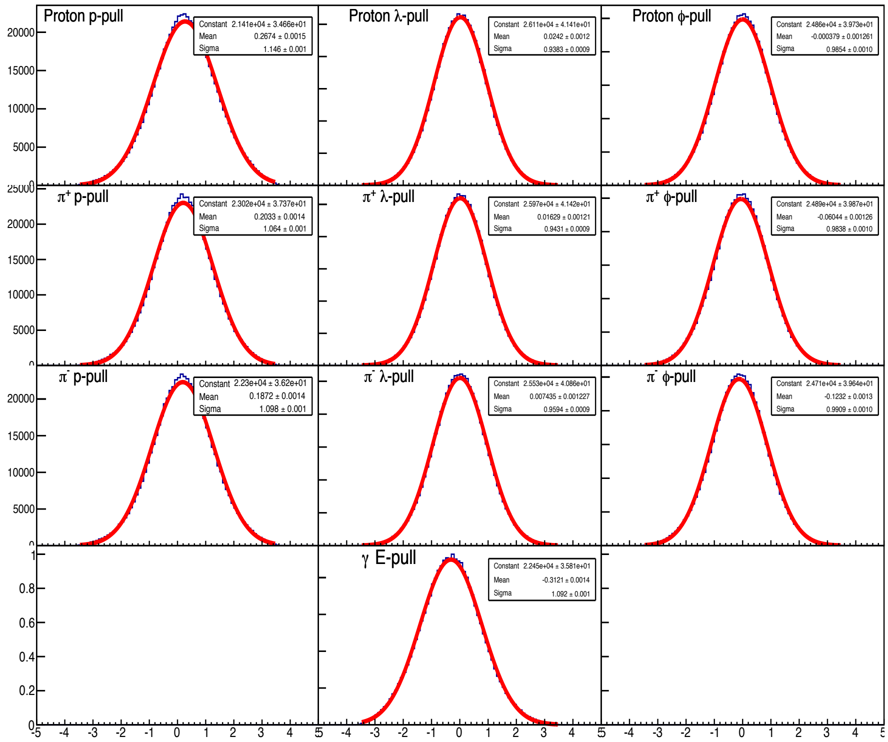

FIGURE 4. The Pull distributions for a (4-C) kinematic fit to $\gamma$ p $\rightarrow$ $\pi^+$ $\pi^-$ p from g12 simulation after a 1% Pull probability cut.

The tuning were done for $\pi^+$ $\pi^-$ and p individually. To check the quality of covariance matrix we have shown the tuned pulls of the particles $\pi^+$, $\pi^-$ and p from the reaction hypothesis for the data with run 56655 and simulation after a 1% pull probability cut. The mean and sigma from of the particles are listed in the Table. 2.

3.1.1. *Fit to the Analysis.* We use the tuned Kinematic fitter for the 4C constrained fit described above to the reaction hypothesis for our channel

$$\gamma p \rightarrow (\eta)_{Missing}\pi^+\pi^- p.$$

We required the $M_x(\mathrm{p}\pi^+\pi^-)$ has to be an $\eta$ meson. Our reaction hypothesis has the same set of final state particles as for the tuned channel, hence we can comfortably use it without tuning it for our reaction hypothesis again. The Pull probability for the channel

(A)

| | $\mu$ | $\sigma$ |
|---|---|---|
| Proton p-pull | 0.187 | 0.846 |
| Proton $\lambda$-pull | -0.029 | 0.928 |
| Proton $\phi$-pull | -0.016 | 1.092 |
| $\pi^+$ p-pull | 0.081 | 0.957 |
| $\pi^+$ $\lambda$-pull | 0.035 | 0.954 |
| $\pi^-$ $\phi$-pull | -0.077 | 1.033 |
| $\pi^-$ p-pull | 0.089 | 0.969 |
| $\pi^-$ $\lambda$-pull | 0.006 | 0.975 |
| $\pi^-$ $\phi$-pull | -0.068 | 1.062 |
| $\gamma$ E-pull | -0.159 | 1.069 |

(B)

| | $\mu$ | $\sigma$ |
|---|---|---|
| Proton p-pull | 0.267 | 1.146 |
| Proton $\lambda$-pull | 0.024 | 0.938 |
| Proton $\phi$-pull | -0.000 | 0.985 |
| $\pi^+$ p-pull | 0.203 | 1.064 |
| $\pi^+$ $\lambda$-pull | 0.016 | 0.943 |
| $\pi^+$ $\phi$-pull | -0.060 | 0.983 |
| $\pi^-$ p-pull | 0.187 | 1.098 |
| $\pi^-$ $\lambda$-pull | 0.007 | 0.959 |
| $\pi^-$ $\phi$-pull | -0.123 | 0.990 |
| $\gamma$ E-pull | -0.312 | 1.092 |

TABLE 2. The table shows the Gaussian mean ($\mu$) and width ($\sigma$) for the pull distributions from a 4C kinematic fit of $\gamma$ p $\rightarrow \pi^+ \pi^-$ to events from (A) data run 56655 and (B) from simulation after a 1% Pull probability cut.

of our interest is shown in Fig. 5 and the dotted line at 0.01 shows the 1% Pull probability cut to reject events.

### 3.2. Simulation

Pluto, an event generator is used for this analysis. Pluto uses ROOT based programmes very commonly used in Hadron Physics experiments to generate hadronic production and decay. It gives user the freedom to include physics models with simple C++ based codes and to obtain outputs in any desired format. Our simulated events are modelled with bremsstrahlung photon, differential cross-section of $\eta'$ and Dalitz plot parameters of $\eta' \rightarrow \eta\, \pi^+ \pi^-$ decay. We took the output of the PLUTO program in standard CLAS "gamp" file and processed it with CLAS simulation suit :

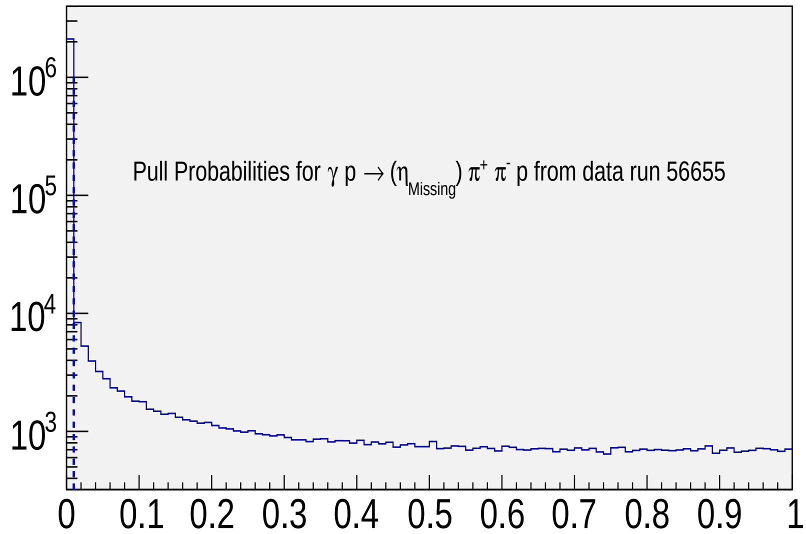


FIGURE 5. The Pull probability for a (1-C) kinematic fit to $\gamma$ p $\rightarrow$ ($\eta_{Missing}$) $\pi^+$ $\pi^-$ p from data run 56655.

- The gamp files are first converted into the format of PART bank containing the event.
- GSIM: Geant3-based simulation in CLAS simulates the decay tracks of particles through the simulation and finally the digitized informations is sorted in the simulated "raw" banks.
- GPP: GSIM post-processor smears detector signal more accurately to reflect the actual resolution and to simulate the experimental conditions.
- a1c : It is used for reconstruction of simulated data and is the same program used during data reconstruction.

The simulated events are then passed through same conditions of Section. 2.3, Section. 2.4, Section. 3 and Section. 3.1. The number of the events rejected in both the simulation and data after the cuts is shown in a Table. 3.

The events are generated with the differential cross sections of $\eta'$ from the g11 measurement [2] within a $|\cos\theta_{center-of-mass}$ of $\eta'| \leq 0.85$. The earlier measurement of CLAS g11 has reported the differential cross sections in $|\cos\theta_{center-of-mass}$ of $\eta'| \leq 0.85$

| Cuts | g12 Run 56655 | Simulation |
|---|---|---|
| Generated | — | 10001500 |
| Reconstructed | 42947 | 855447 |
| Vertex Cut | 20092 | 505405 |
| Timing Cut | 11390 | 451470 |
| Multiple $E_\gamma$ | 14986 | — |
| Fiducial Cuts | 10541 | 276432 |
| Prob(($\eta$)$\pi^+\pi^-$p) >0.01 | 1901 | 259136 |

TABLE 3. The table shows the cut flow of the analysis from g12 data run 56655 and simulated events.

window as the yield drops near to the beam pipe and hence this region is removed from the analysis. The generated events also has the input Dalitz plot parameters from BESIII measurement [3]. A comparison of the kinematic variables of the center-of-mass energy ($\sqrt{s}$) and momentum (P), $\theta$ and $\phi$ for $\pi^+$ $\pi^-$ and p is shown in the Figure. 6, 7, 8 & 9 from the simulated events and the g12 data.

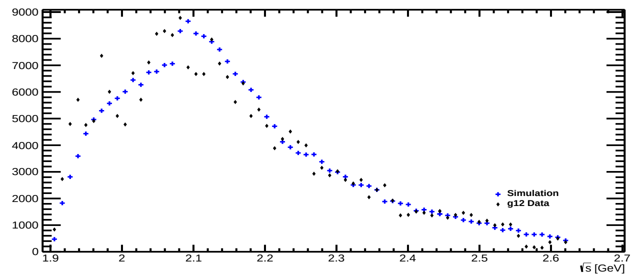


FIGURE 6. Comparison of incident photon beam in center of mass energy ($\sqrt{s}$) with simulated (blue) events and g12 data (black) when generating Monte-Carlo with the differential cross-sections and Dalitz plot parameters.

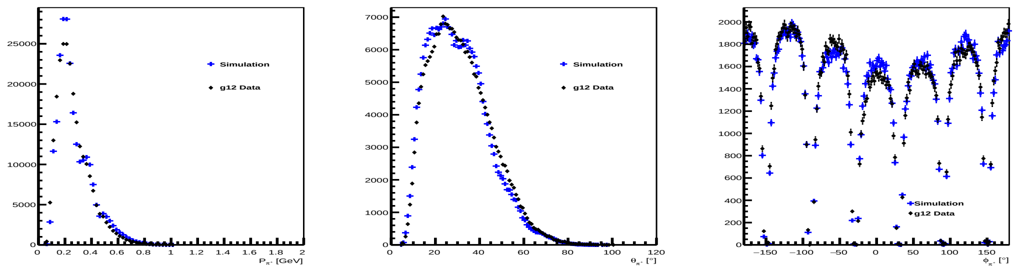


FIGURE 7. Comparison of $\pi^+$ momentum (top), $\pi^+$ $\theta$ (middle) and $\pi^+$ $\phi$ (bottom) with simulated (blue) events and g12 data (black) when generating Monte-Carlo with the differential cross-sections and Dalitz plot parameters.

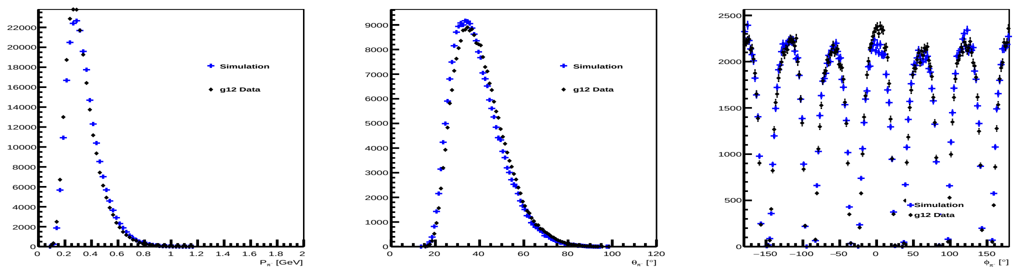


FIGURE 8. Comparison of $\pi^-$ momentum (top), $\pi^-$ $\theta$ (middle) and $\pi^-$ $\phi$ (bottom) with simulated (blue) events and g12 data (black) when generating Monte-Carlo with the differential cross-sections and Dalitz plot parameters.

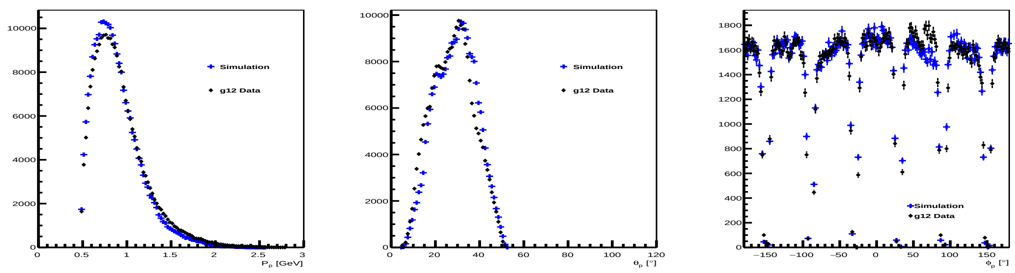


FIGURE 9. Comparison of proton momentum (top), proton $\theta$ (middle) and proton $\phi$ (bottom) with simulated (blue) events and g12 data (black) when generating Monte-Carlo with the differential cross-sections and Dalitz plot parameters.

# 4. Dalitz plot of $\eta' \to \eta\ \pi^+\ \pi^-$

The three body decay of a meson has two degrees of freedom. So we can define a scatter plot with two Dalitz plot variables X and Y for $\eta' \to \eta\ \pi^+\ \pi^-$ decay, which is defined as follows:

$$X = \frac{\sqrt{3}(T_{\pi^+} - T_{\pi^-})}{Q} \quad (1)$$

$$Y = \frac{(m_\eta + 2m_\pi)}{m_\pi} \cdot \frac{T_\eta}{Q} - 1. \quad (2)$$

Where $T_\eta$, $T_{\pi^+}$ and $T_{\pi^-}$ are the kinetic energy of a given particles $\eta$, $\pi^+$ and $\pi^-$ respectively in the rest frame of $\eta'$ and Q = $T_{\pi^+}$+$T_{\pi^-}$+$T_\eta$. The $m_\eta$ and $m_\pi$ are the mass of $\eta$ and $\pi$ mesons respectively.

One can also define the boundary of the $\eta' \to \eta\ \pi^+\ \pi^-$ decay from the fact that the addition three momenta of particles $\vec{P}_\eta$, $\vec{P}_{\pi+}$ and $\vec{P}_{\pi-}$ for $\eta$, $\pi^+$ and $\pi^-$ respectively is 0 in the rest frame of $\eta'$.

$$\vec{P}_\eta + \vec{P}_{\pi+} + \vec{P}_{\pi-} = 0.$$

Squaring and equating the side gives us the boundary Equation. 3 of the $\eta' \to \eta\ \pi^+\ \pi^-$ decay.

$$|{P_\eta}^2 - {P_{\pi+}}^2 - {P_{\pi-}}^2| \leq 2\vec{P}_{\pi+}.\vec{P}_{\pi-} \quad (3)$$

## 4.1. Fit to the Dalitz Plot

Once we the $\eta' \to \eta\ \pi^+\ \pi^-$ events filled in each bin of Dalitz plot. We fit the Dalitz plot with the general parametization function in Equation. 4. The square of the decay amplitude,

$$M^2 = A(1 + aY + bY^2 + cX + dX^2). \quad (4)$$

Where a, b, c, and d are the Dalitz plot parameters of the decay and A is the normalization constant.

The fitting is performed using the least square fitting procedure and MINUIT available in ROOT, which minimises the $\chi^2$ using Equation. 5 in each bin of the Dalitz plot.

$$\chi^2 = \sum_{n=1}^{Nbins} \left( \frac{N_n - \sum_{m=1}^{Nbins} \epsilon_{n,m} N_{theory,m}}{\sigma_n} \right)^2 \tag{5}$$

Where,

- The $N_n$ is number of $\eta' \rightarrow \eta\ \pi^+\ \pi^-$ events in the $n^{th}$ Dalitz plot bin.
- $\epsilon_{n,m}$ is acceptance with smearing matrix, ie. it gives acceptance of $m^{th}$ bin when events are generated in the n$^{th}$ bin only.
- $N_{theory,m} = \int_{Boundary}$ A(1 + aY + b$Y^2$ + cX + d $X^2$) dX dY.
- $\sigma_n$ is the error associated with $n^{th}$ DP bin.

# REFERENCES


[1] Z. Akbar et al. g12 Analysis Procedures, Statistics and Systematics. Technical report, CLAS Technical Note, 2016.

[2] M. Williams *et al.* [CLAS Collaboration], Phys. Rev. C **80**, 045213 (2009)

[3] M. Ablikim *et al.* [BESIII Collaboration], Phys. Rev. D **83**, 012003 (2011)